

Supplementary Information

Molecular self-assembly of a nanorod-like $N\text{-Li}_4\text{Ti}_5\text{O}_{12}/\text{TiO}_2/\text{C}$ anode for superior lithium ion storage

Sainan Luo^{a,1}, Pengcheng Zhang^{a,1}, Tao Yuan^{a,b,*}, Jiafeng Ruan^a, Chengxin Peng^{a,b}, Yuepeng Pang^{a,b}, Hao Sun^{a,b}, Junhe Yang^{a,b}, Shiyong Zheng^{a,b,*}

^a School of Materials Science and Engineering, University of Shanghai for Science and Technology, Shanghai 200093, China

^b Shanghai Innovation Institute for Materials, Shanghai 200444, China

* Corresponding author at: School of Materials Science and Engineering, University of Shanghai for Science and Technology, Shanghai 200093, China

E-mail addresses: E-mail: yuantao@usst.edu.cn (T. Yuan), syzheng@usst.edu.cn (S. Zheng).

¹ These authors contributed equally to this work.

Contents:

Figure S1. TGA curve for the NT-LTO/C composite in an air atmosphere with a heating rate of $10\text{ }^{\circ}\text{C min}^{-1}$.

Figure S2. TEM photographs of pristine LTO with mechanical mixing of anatase-TiO₂ and LiOH as reactants after calcination at $750\text{ }^{\circ}\text{C}$ for 5 h in a N₂ atmosphere.

Figure S3. (a) CV curves from 0.2 to 10 mV s^{-1} ; (b) analysis of b -value for anodic and cathodic peak currents; (c) The plots of $v^{1/2}$ vs $i/v^{1/2}$ used for calculating constants k_1 and k_2 at different potentials; (d) capacitive (red) and diffusion currents contributed to charge storage of NT-LTO/C at a scan rate of 1 mV s^{-1} .

Figure S4. The discharge and charge profiles for the pristine LTO electrode at various rates from 0.5 C to 100 C.

Figure S5. The relationship of the voltage vs. x in NT-LTO/C and LTO electrodes.

Figure S6. Real and imaginary parts of the complex impedance vs. $\omega^{-1/2}$ for the NT-LTO/C and LTO electrodes.

Figure S7. The corresponding cathode and anode curves during the charge/discharge process of LFP||pristine LTO cell.

Table S1. Refined structural parameters of Li₄Ti₅O₁₂ obtained from the two phase Rietveld refinement using X-ray powder diffraction data at room temperature. The symbols, g and U , represent the occupation and isotropic thermal parameters, respectively. The profile factor is R_p , and the weighted profile factor is R_{wp} .

Table S2. Ratio analysis of the peaks in the XPS spectrum of the NT-LTO/C composite

Table S3. Ti2p composition from XPS

Table S4. N1s composition from XPS

Table S5. Values of A , dE/dx and the diffusion coefficient D of NT-LTO/C and LTO electrodes at a discharge voltage of 2.0 V.

Figure S1

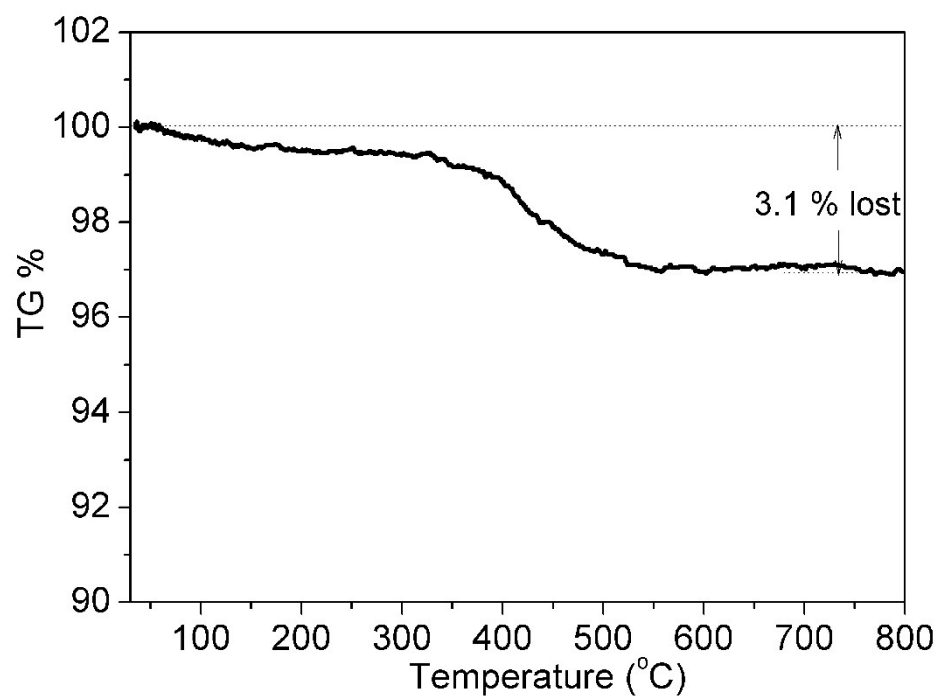


Figure S1 TGA curve for the NT-LTO/C composite in an air atmosphere with a heating rate of 10 °C min⁻¹.

Figure S2

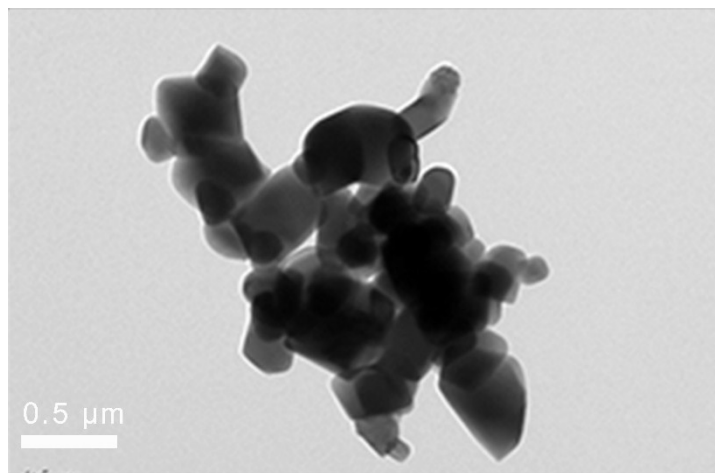


Figure S2 TEM photographs of pristine LTO with mechanical mixing of anatase-TiO₂ and LiOH as reactants after the calcination at 750 °C for 5 h in a N₂ atmosphere.

Figure S3

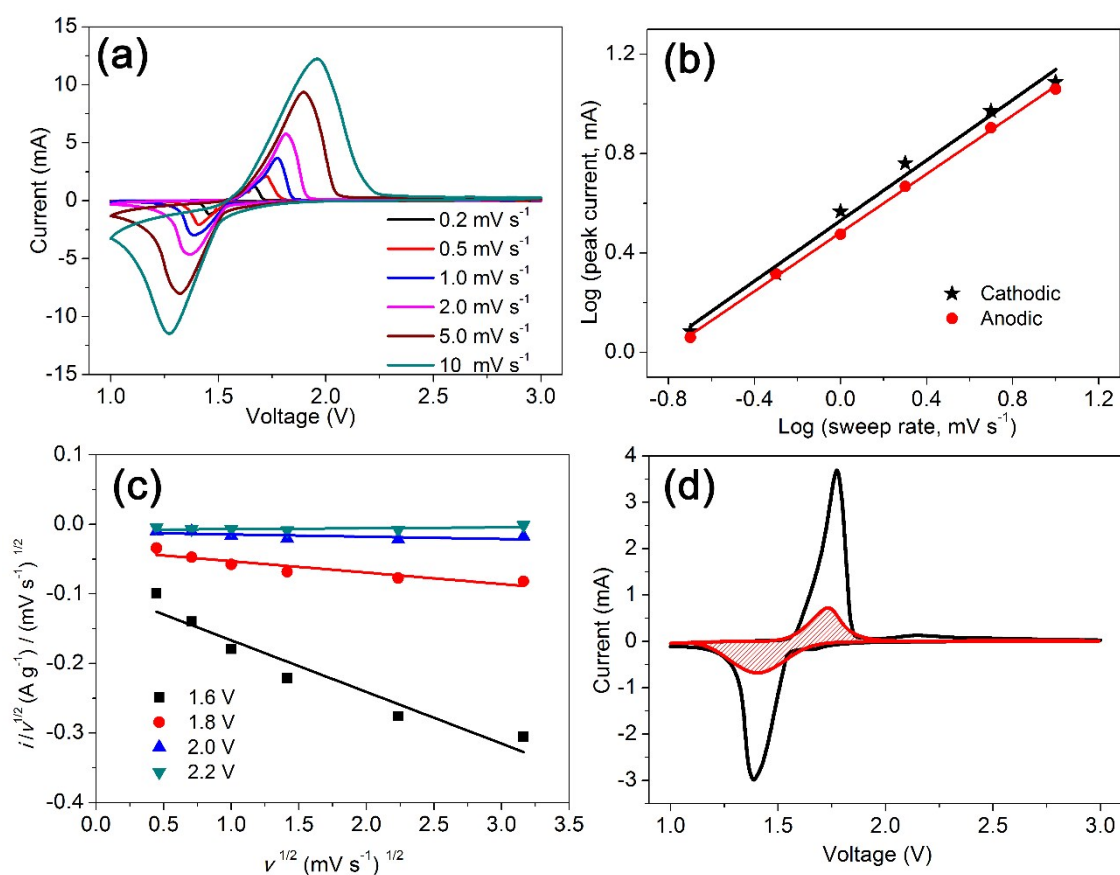


Figure S3. (a) CV curves from 0.2 to 10 mV s⁻¹; (b) analysis of b -value for anodic and cathodic peak currents; (c) The plots of $v^{1/2}$ vs $i/v^{1/2}$ used for calculating constants k_1 and k_2 at different potentials; (d) capacitive (red) and diffusion currents contributed to charge storage of NT-LTO/C at a scan rate of 1 mV s⁻¹.

To investigate the pseudocapacitance performance of the NT-LTO/C electrode, the ion diffusion and charge storage kinetics of NT-LTO/C electrode are investigated by CV at various scan rates from 0.2 to 10 mV s⁻¹ (**Figure S3a**). **Equation S1** describes the kinetic mechanism by the dependence of the current (i) on the scan rate (v).¹

$$i = av^b \quad (\text{Eq. S1})$$

where, b value is an adjustable parameter, which represents the slope of the $\log(v)$ – $\log(i)$ plots. Typically, the slope of 0.5 ($b=0.5$) signifies a diffusion-controlled process, and the slope of 1 ($b=1$) suggests a capacitive-controlled behavior (also named surface Faradic redox reaction).² As displayed in **Figure S3b**, the cathodic and anodic b values of NT-LTO/C anode in LIBs are 0.61 and 0.59 respectively, demonstrating that the ion storage mechanism of NT-LTO/C anode tends to both diffusion-controlled and capacitive-controlled processes. Moreover, the contribution ratios of diffusion-controlled processes and capacitive-controlled process are quantitatively separated through the method by Dunn and co-workers:³

$$i = k_1v + k_2v^{1/2} \quad (\text{Eq. S2})$$

In **Equation S2**, k_1v and $k_2v^{1/2}$ represent the surface capacitive and diffusion-controlled process, respectively.^{4,5} The current at a fixed potential (i) can be expressed as a combination of k_1v and $k_2v^{1/2}$. By plotting $i/v^{1/2}$ versus $v^{1/2}$ (**Figure S3c**), one can determine k_1 and k_2 from the slope and the y-axis intercept point of a straight line, respectively. Comparing the shaded area (k_1v) in **Figure S3d**, it can be found that ~30.5 % of the total charge in the NT-LTO/C electrode is surface capacitive (red region) at a scan rate of 1 mV s⁻¹. This result suggests that the NT-LTO/C electrode is dominated by pseudocapacitive nature during the charge/discharge process.

Figure S4

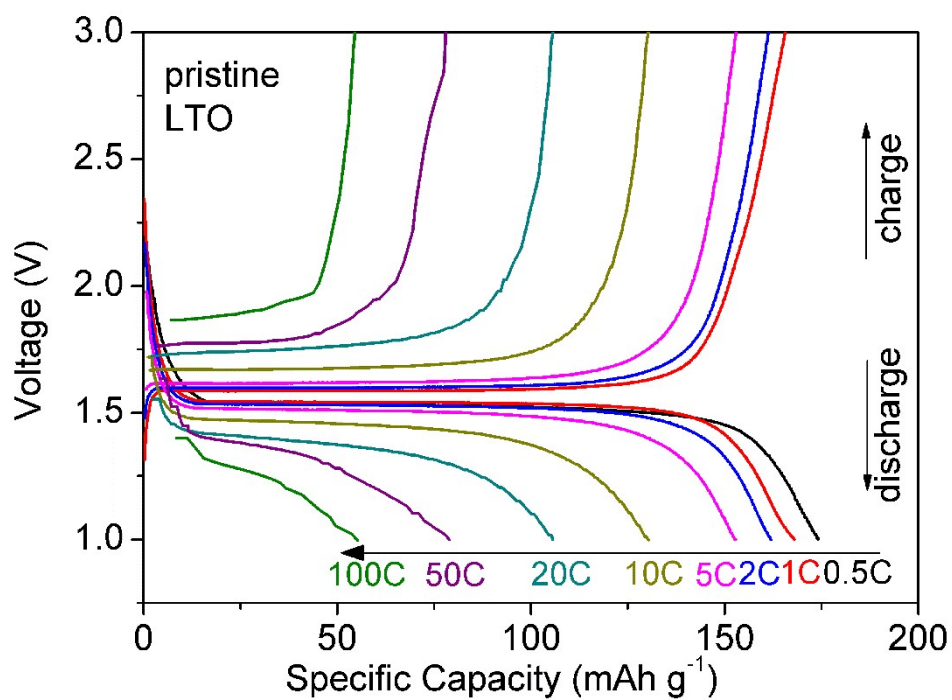


Figure S4 The discharge and charge profiles for the pristine LTO electrode at various rates from 0.5 C to 100 C.

Figure S5

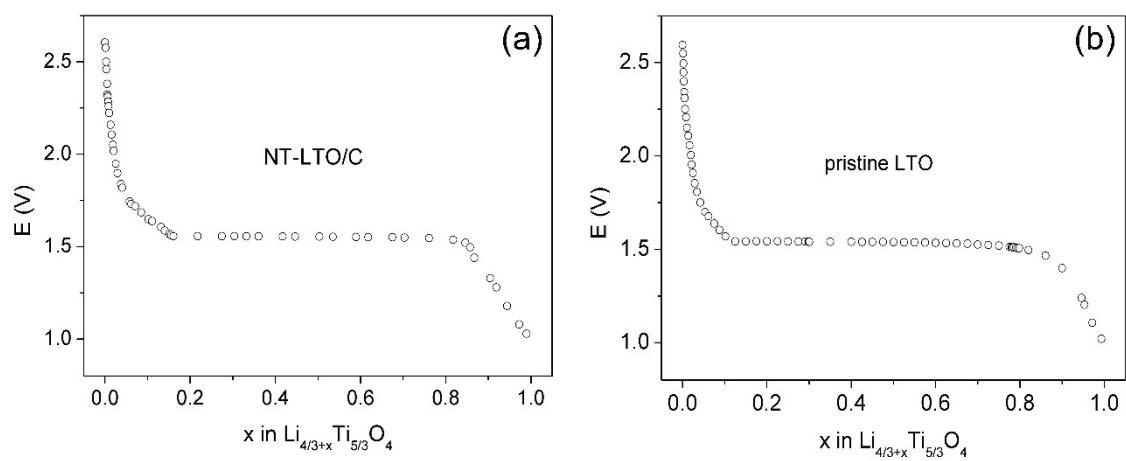


Figure S5 The relationship of the voltage vs. x in NT-LTO/C and LTO electrodes.

Figure S6

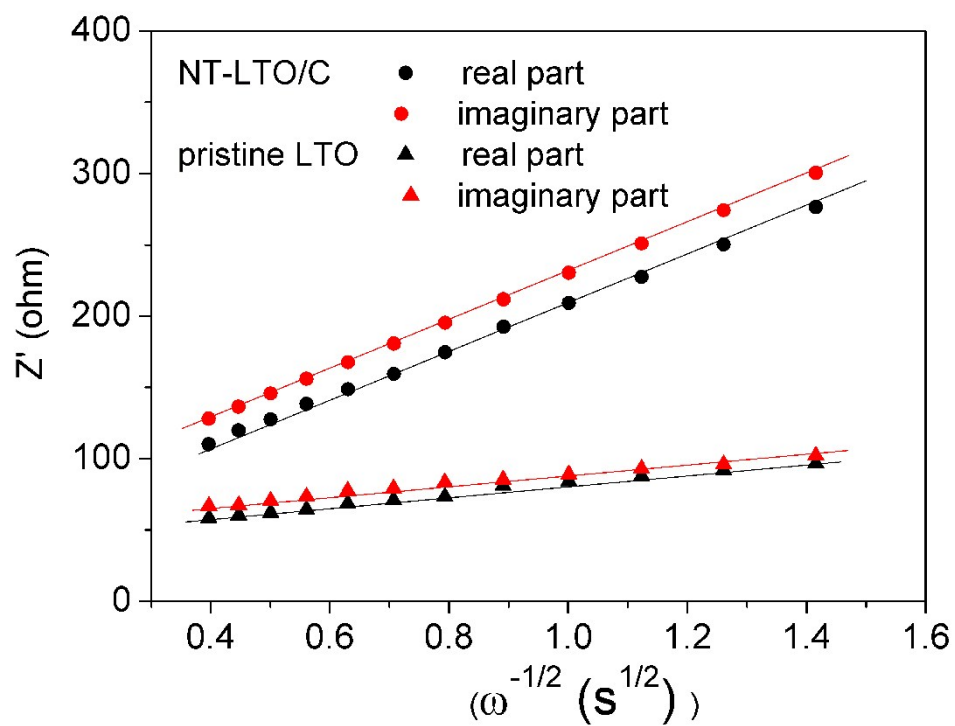


Figure S6 Real and imaginary parts of the complex impedance vs. $\omega^{-1/2}$ for the NT-LTO/C and LTO electrodes.

Figure S7

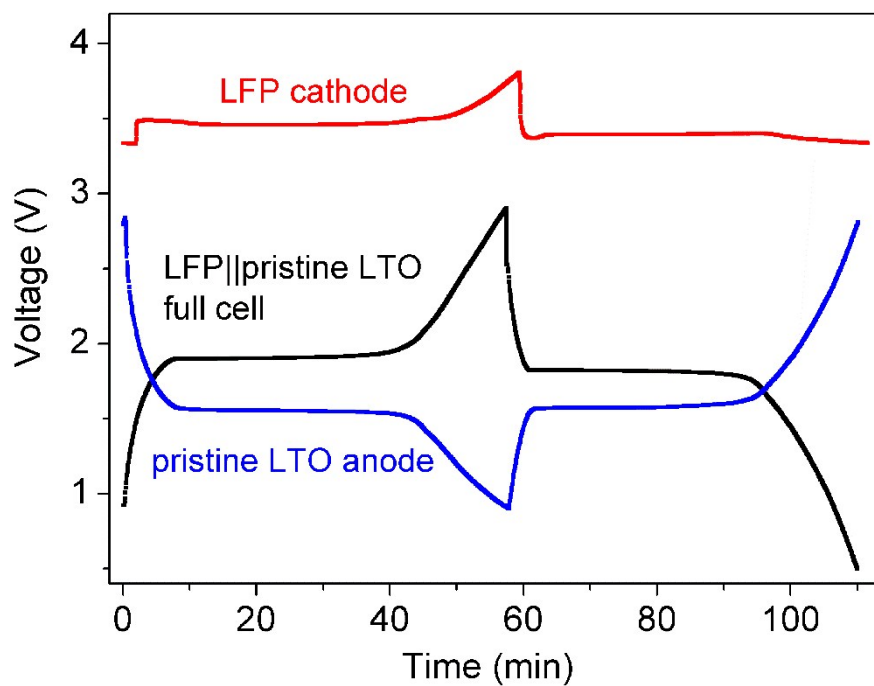


Figure S7 The corresponding cathode and anode curves during the charge/discharge process of the LFP||pristine LTO cell.

Table S1 Refined structural parameters of $\text{Li}_4\text{Ti}_5\text{O}_{12}$ obtained from the two phase Rietveld refinement using X-ray powder diffraction data at room temperature. The symbols, g and U, represent the occupation and isotropic thermal parameters, respectively. The profile factor is

R_p , the weighted profile factor is R_{wp} .

$\text{Li}_4\text{Ti}_5\text{O}_{12}$ (phase No. 1)						
Atom	site	x	Y	z	g	U
Li	8a	0.0000	0.0000	0.0000	1.000	0.0000
Li	16c	0.6250	0.6250	0.6250	0.1667	0.0000
Ti	16c	0.6250	0.6250	0.6250	0.8333	0.0000
O	32e	0.3890	0.3890	0.3890	1.0000	0.0000
a=8.357 Å b=8.357 Å c=8.357 Å $\alpha=\beta=\gamma=90^\circ$						
TiO_2 (phase No. 2)						
Atom	site	x	y	z	g	U
Ti	4a	0.0000	0.7500	0.1250	1.0000	0.0000
O	8e	0.0000	0.7500	0.3333	1.0000	0.0000
a=3.785 Å b=3.785 Å c=9.514 Å $\alpha=\beta=\gamma=90^\circ$						
R-factors and weight fraction						
$R_{wp} = 9.77\%$ $R_p = 7.26\%$ $S = 1.5914$						
$\text{Li}_4\text{Ti}_5\text{O}_{12} : 95.48\%$ $\text{TiO}_2 : 4.52\%$						

Table S2 Ratio analysis of the peaks in the XPS spectrum of the NT-LTO/C composite

	Ratios (% at.)				
	Li	Ti	O	C	N
NT-LTO/C	11.3	36.6	38.7	11.0	2.4

Table S3 Ti2p composition from XPS

	Ti ⁴⁺ 2p _{1/2}	Ti ³⁺ 2p _{1/2}	Ti ⁴⁺ 2p _{3/2}	Ti ³⁺ 2p _{3/2}
Binding Energy (eV)	464.3	463.1	458.4	457.2
Ratios (% at.)	14.41	14.57	47.96	23.06

Table S4 N1s composition from XPS

peaks	N4	N3	N2	N1	TiN
Nitrogen atom components	High-oxidation states-N	Protonated-N	Pyrrolic-N	Pyridinic-N	TiN
Binding Energy (eV)	401.3	400.3	399.5	398.81	397.5
Ratios (atomic %)	12.2	33.4	12.5	5.0	36.9

Table S5 Values of A , dE/dx and the diffusion coefficient D of NT-LTO/C and LTO electrodes at a discharge voltage of 2.0 V.

Electrodes	A	dE/dx	D (cm ² s ⁻¹)
C-LTO	28.22	15.957	3.01×10^{-12}
LTO	163.22	7.422	1.94×10^{-14}

The chemical diffusion coefficients of Li⁺ inside NT-LTO/C and LTO electrodes can be estimated from the impedance results. The following expression for Z_w was derived by solving Fick's law:⁶

$$Z_w = A\omega^{-1/2} - jA\omega^{-1/2} \quad (\text{Eq. S3})$$

$$A = \frac{V_M(dE/dx)}{\sqrt{2zFD^{1/2}a}} \quad (\text{Eq. S4})$$

where, ω is the frequency, $j = \sqrt{-1}$, and the pre-exponential factor A is a constant that contains a concentration independent chemical diffusion coefficient, as shown in **Equation S4**. V_M is the molar volume of LTO (45.73 cm³ mol⁻¹), dE/dx values are the slope of the NT-LTO/C and LTO electrode potential curves vs. x in **Figure S5**, z is the charge transfer number ($z=1$ in the lithium intercalation reaction), a is the electroactive surface area of the electrode, which is

1.13 cm² in our testing electrode, F is the Faraday constant, and D is the diffusion coefficient. **Figure S6** displays the dependence of the impedances on the frequencies of the NT-LTO/C and LTO electrodes. Both the real and imaginary parts of the impedance were found to be parallel to each other, and proportional to $\omega^{-1/2}$. Based on the slope of the plot, the value of A was obtained. Since A is inversely proportional to the chemical diffusion coefficient, D , as demonstrated in **Equation S4**, the larger A , the slower the diffusion rate of Li⁺ in the solid matrix of the electrode should be. **Table S5** lists the values of the dE/dx , A and D of NT-LTO/C and LTO electrodes. The chemical diffusion coefficients of the NT-LTO/C and LTO electrodes are 3.01×10^{-12} cm² s⁻¹ and 1.94×10^{-14} cm² s⁻¹, respectively.

References

1. M. Sathiya, A. S. Prakash, K. Ramesha, J. M. Tarascon, A. K. Shukla, *J. Am. Chem. Soc.*, 2011, 133, 16291-16299.
2. Y. Zhou, X. Rui, W. Sun, Z. Xu, Y. Zhou, W. J. Ng, Q. Yan, E. Fong, *ACS Nano*, 2015, 9, 4628-4635.
3. J. Wang, J. Polleux, J. Lim, B. Dunn, *J. Phys. Chem. C*, 2007, 111, 14925-14931.
4. R. Wang, S. Wang, D. Jin, Y. Zhang, Y. Cai, J. Ma, L. Zhang, *Energy Storage Materials*, 2017, 9, 195-205.
5. H. Wang, Y. Zhang, H. Ang, Y. Zhang, H.T. Tan, Y. Zhang, Y. Guo, J. B. Franklin, X. L. Wu, M. Srinivasan, H. J. Fan, Q. Yan, *Adv. Funct. Mater.*, 2016, 26, 3082-3093.
6. T. Yuan, X. Yu, R. Cai, Y.K. Zhou, Z.P. Shao, *J. Power Sources*, 2010, **195**, 4997-5004.